3

Structure and Stability of Emulsions

Darsh T. Wasan Alex D. Nikolov
Illinois Institute of Technology, Chicago, Illinois

Emulsion stability is characterized in different ways—creaming or sedimentation, fiocculation of drops, coalescence between drops, or phase separation. A number of novel experimental techniques have been developed in our laboratory to examine both the structure and stability of emulsions. This chapter highlights our more recent experimental methods which include: (Sec. I) film rheometry for dynamic film properties; (Sec. II) capillary force balance in conjunction with differential microinterferometry for drainage of curved emulsion films; (Sec. Ill) back-light scattering (Kossel diffraction) for structure factor; (Sec. IV) direct imaging for effective interdroplet interactions; and (Sec. V) piezo imaging spectroscopy for drop-homophase coalescence-rate processes. These experimental techniques are being used by us to gain a mechanistic understanding of both the structure and stability of polydisperse emulsion and foam systems (1—7).

I. FILM RHEOMETRY

The stability of any emulsion is largely due to the nature of the film that is formed between two approaching droplets. Coalescence of drops in any emulsion system is a dynamic process. The rheological behavior of emulsions depends on the response of the thin liquid films and the plateau borders during shear and dilation. In real emulsions, the size and distribution of the drops is generally poly disperse. Hence, thin liquid films formed between drops are typically not flat, as in a homogeneous dispersion, but have a spherical, curved shape due to the capillary pressure difference between drops of unequal size.

A versatile interfacial and film rheometer has been developed in our laboratory (7—10). In this technique, a curved, spherical cap-shaped fluid interface or liquid film is formed at a capillary tip and the interfacial tension (IFT) of the single interface or the film tension of the film can be determined by measuring the capillary pressure of the interface or film (Fig. 1). The IFT or film tension is related to the capillary pressure and the radius of the interface or film curvature by the Young-Laplace equation. The IFT and film tension can be measured not only in equilibrium, but also in dynamic conditions as well. The automated apparatus makes it possible to change the interfacial or film area in virtually any mode (expansion or contraction) at various rates (Fig. 2). This instrument is now made available through our laboratory.

The flocculation and coalescence processes of a polydispersed lamella or film can be divided into two processes: film drainage and film rupture. To model the film-rupture process of polydispersed emulsions, film stress-relaxation experiments were carried out. In these experiments, the film was quickly expanded and then the relaxation of the film was measured. To characterize the film-drainage process, dynamic film-tension measurements were conducted in which the film was continuously and slowly expanded while the film tension was monitored. Single interfaces were also studied by forming a drop at the capillary (7).
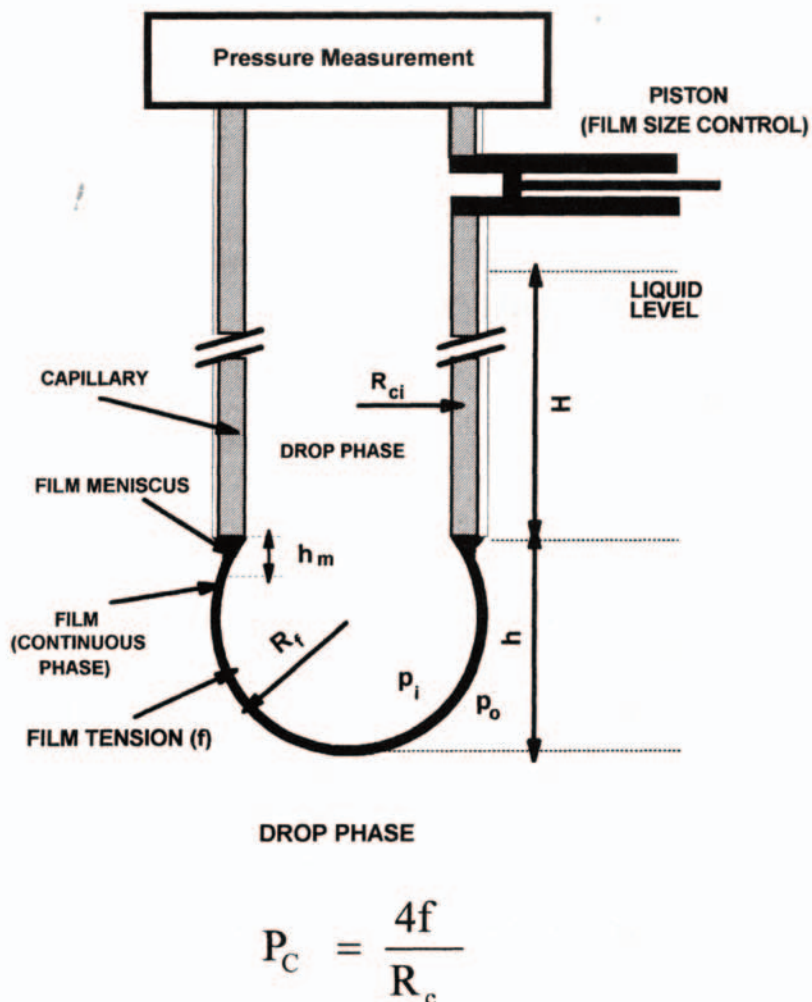
59

Figure 1 Principle of studying liquid film formed at the tip of a capillary.

Figure 3 shows a film stress-relaxation experiment with an aqueous emulsion film formed between dodecane drops. The film was suddenly expanded by 22% in area and then the film size was kept constant. The stress-relaxation curve provides information about the kinetics of emulsifier adsorption on the film surfaces. Figure 3 also shows that the repro-ducibility of the film stress-relaxation experiment was very good.

In the dynamic film-tension experiments, the film area is continuously increased by a constant rate and the dynamic film tension is monitored. The measured film tensions were compared with the interfacial tensions of the oil/water interfaces. It was found that under dynamic conditions, the film tension is higher than twice the single interfacial tension (Fig. 4). These results have important implications for the stability and rheology of emulsions with high disperse phase ratios (polyhedral structure).

The initial (maximum) film tension after the expansion in the film stress-relaxation experiments can also be used to determine the film elasticity (7). A plot of the initial film tension versus the logarithm of the relative film expansion is shown in Fig. 5. For comparison, the initial single interfacial tensions obtained in the experiments with the respective single oil/water interface are also plotted. The film elasticity obtained from the top of the curve is equal, within experimental error, to twice the interfacial elasticity of the single interface.
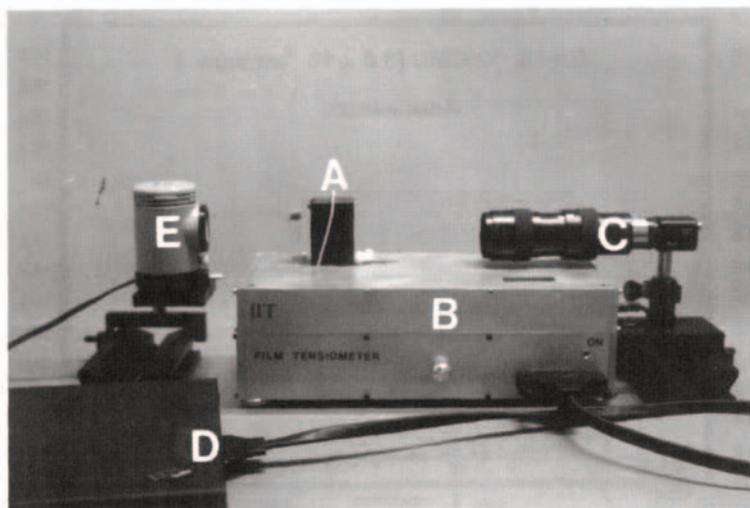
Figure 2 Photograph of our new film rheometer: (A) capillary with capillary holder; (B) operation control; (C) zoom objective with camera; (D) computer; (E) light illuminator.

II. CAPILLARY FORCE BALANCE

We have constructed a new surface-force apparatus capable of measuring the capillary pressure and structural disjoining pressure of the thinning curved emulsion film as a function of time and film thickness (11-16). This apparatus is equipped with Max Zhender differential interferometry (DI) which is used to measure the film curvature (2). A sketch of the surface-force balance experimental set-up is shown in Fig. 6. For measuring oil-in-water emulsions the inner capillary of the cell is filled with oil phase, the bottom part of the outer capillary is filled with water phase, and the top part of the outer capillary if filled with oil phase. A curved film is formed by drawing the oil phase from the
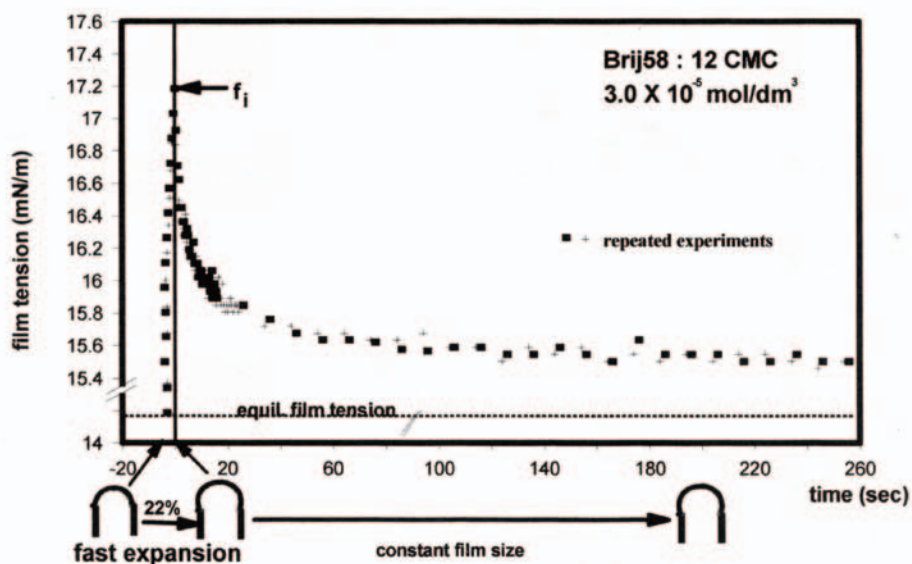
Figure 3 Reproducibility of the film stress-relaxation experiment for the aqueous emulsion film stabilized with 3.0×10^5 mol/ dm^3 (12 CMC) Brij 58.
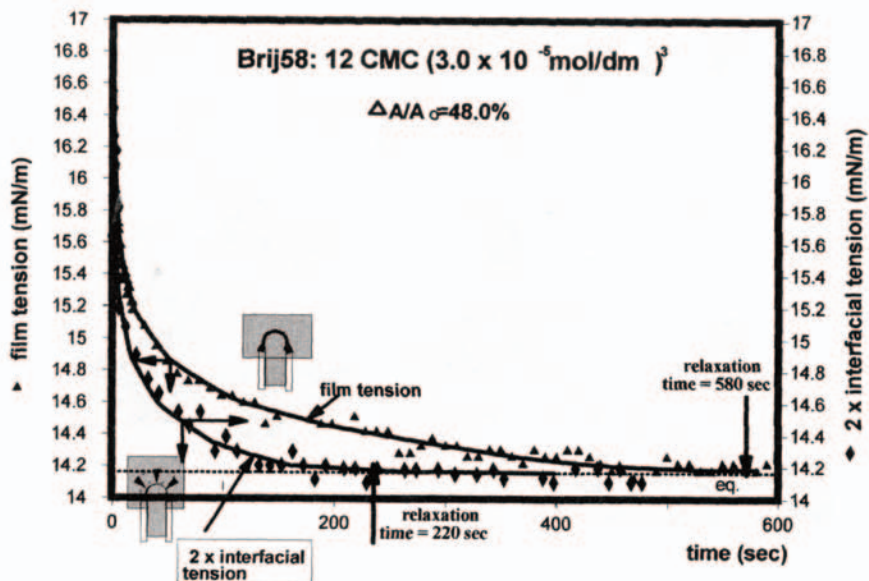
Figure 4 Comparison of the relaxation of film tension and single interfacial tension (IFT) with 48% relative expansion of the emulsion system with 3.0×10^{-5} mol/dm^3 Brij 58 (< 1 CMC).

inner capillary, using a piston pump. The film curvature can be varied by changing the ratio of the outer to inner capillary diameter.

Also, we have recently used the capillary force balance in conjunction with reflected-light microinterferometry to study stratification (i.e., micelles ordered in layers) phenomena inside emulsion films, which is one of the key mechanisms controlling film stability (4, 11-16). Figure 7 shows a photocurrent versus time inter-ferogram of the film-thinning process in a microscopic horizontal film (film diameter 3.6×10^{-2}cm) stabilized by sodium dodecyl sulfate (6×10^{-2}M). The thickness at which the stepwise transition
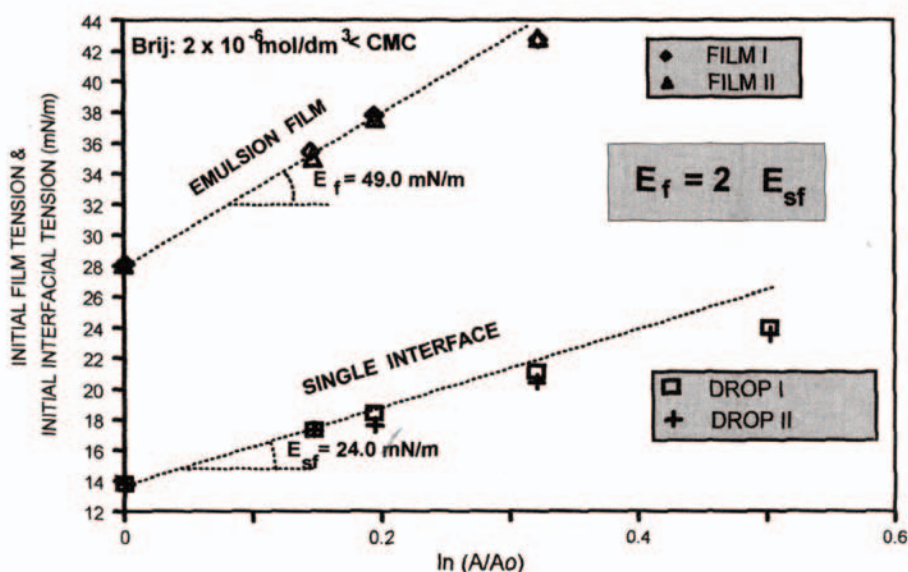
Figure 5 Initial film tension and IFT in the stress-relaxation experiments as a function of $\ln(A/A_O)$ for the emulsion system, in the presence of 2.0×10^{-6} mol/dm^3 Brij 58 (< 1 CMC).
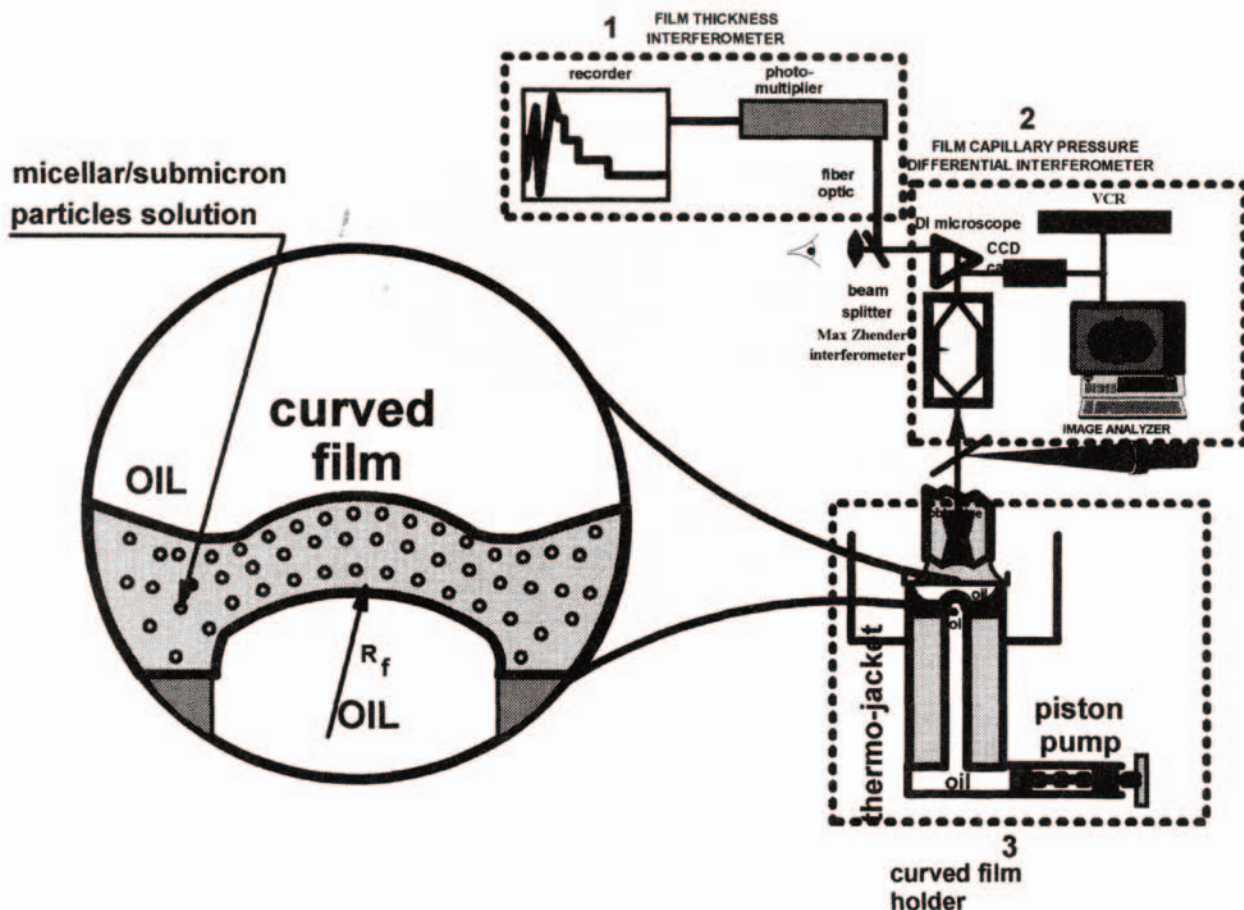
Figure 6 Capillary force balance.

begins is marked with an arrow. The system consists of an oil-in-water type emulsion. In this case, the water film changes its thickness only once, and at this thickness, the film contains three layers of micelles. The final film contains two layers of micelles and is stable.

Figure 8 shows photomicrographs of the various stages of stepwise thinning of a microscopic, horizontal oil film stabilized by asphaltene particles (7 vol%) in a 1:1 volume mixture of n-heptane and toluene. At a film thickness greater than about 300-nm, the asphaltene particles inside the film form a random structure which causes the white and dark interference patterns produced in reflected monochromatic light to form a mosaic structure (Fig. 8a). The film is irregular. After a while, a white expanding spot surrounded by a dark rim appears inside the film with a thickness of about 100-nm (Fig. 8b). Here, one can see that the film thickness at the spot area appears to be much more reg-

ular than the surrounding film. Subsequently, the spot expands (Fig. 8c, d) and, finally, the white spot occupies the whole film.

We have also observed the dynamic film-thickness transition phenomenon (i.e. stratification), inside an ice-cream emulsion film, caused by layering of caseinate submicelles inside it (13).

The investigations in our laboratory showed that the film microlayering was a universal phenomenon (17, 18) which fundamentally differed from the classical film-thinning mechanism by the common black film/ Newton film transition. The particles may be any kind of isotropic structures in the 10-100-nm range including micelles, fine solid particles, globular protein molecules, or random coil-shaped polysaccharide molecules or protein aggregates such as caseinate submicelles. This ordering occurs because highly charged Brownian particles (micelles) interact via repulsive
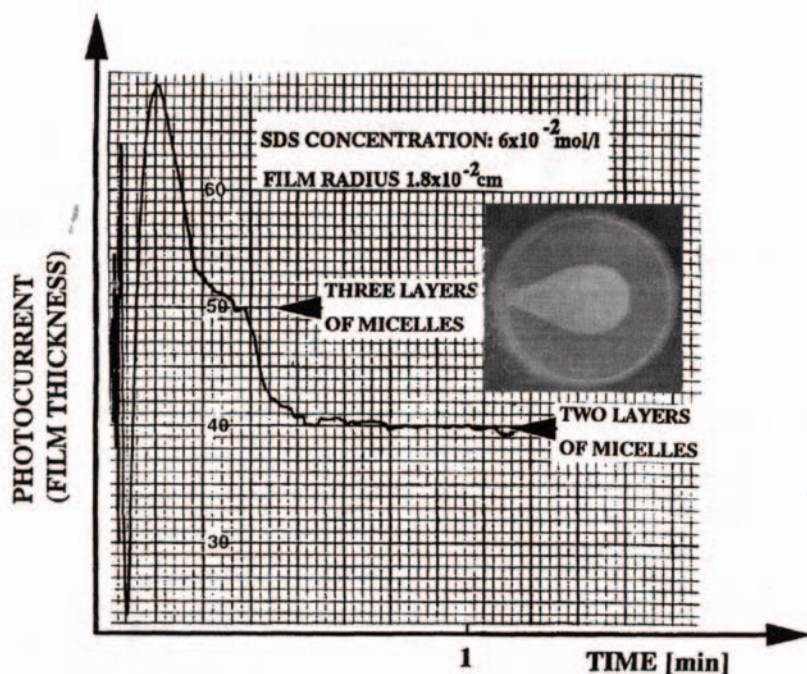
Figure 7 Photocurrent vs. time interferogram of thinning of the emulsion film of sodium dodecyl sulfate. The photomicrograph depicts the moment of film thickness transition from three to two micellar layers.

forces inside the restricted volume of the film. The classical Derjaguin, Landau, Verwey, Overbeck (DLVO) theory of colloid stability, which explains order in colloidal systems as a balance of van der Waals attractive forces and electrostatic forces, cannot be used here because the intermicellar distances are too large for the van der Waals forces to be sufficiently significant to balance the respulsive forces (19, 20).

We have investigated theoretically film-thickness stability and structure formation inside a liquid film by Monte Carlo numerical simulations and analytical methods, using the Ornstein-Zernicke (O-Z) statistical mechanics theory (21-24). The formation of longrange, ordered microstructures (giving rise to an oscillating force) within the liquid film leads to a new mechanism of stabilization of emulsions (3, 4, 25). In addition to the effective volume of micelles or other colloidal particles and polydispersity in micelle size, the film size is also found to be the main parameter governing emulsion stability (15).

III. BACK-LIGHT SCATTERING—-KOSSEL DIFFRACTION

This optical technique can be used to investigate the structure and texture of emulsions. In the method, the emulsion, in a transparent vessel, is illuminated by a collimated laser beam. A portion of the light rays are scattered from the emulsion droplets through the wall of the vessel and form a concentric interference pattern (26). The back-scattering phenomenon is analogous to the operation of diffraction gratings. The measurement can be used to characterize the packing structure of the emulsion. The average pair potential (potential of mean force), which is the potential (free) energy of a pair of droplets in the presence of other droplets, can be calculated from the radial distribution function.

Figure 9 shows the structure factor as a function of the light-scattering vector depicting the fat particle structure inside the food emulsion. There are two samples shown in this figure. The two samples included the same fat concentration (5.14 wt%) except that the caseinate concentration inside sample 4 was half of that inside sample 1. The first peak height of structure factor $S(a)$ of the sample with higher caseinate concentration was higher, indicating that the addition of caseinate facilitates fat-particle structure formation. This could be explained by the stabilization mechanism of caseinate submicelles in the aqueous phase (13). Results for a binary system consisting of fat particles and caseinate submicelles were calculated by us from the O-Z equation (Fig.10. The parameters used in these calculations
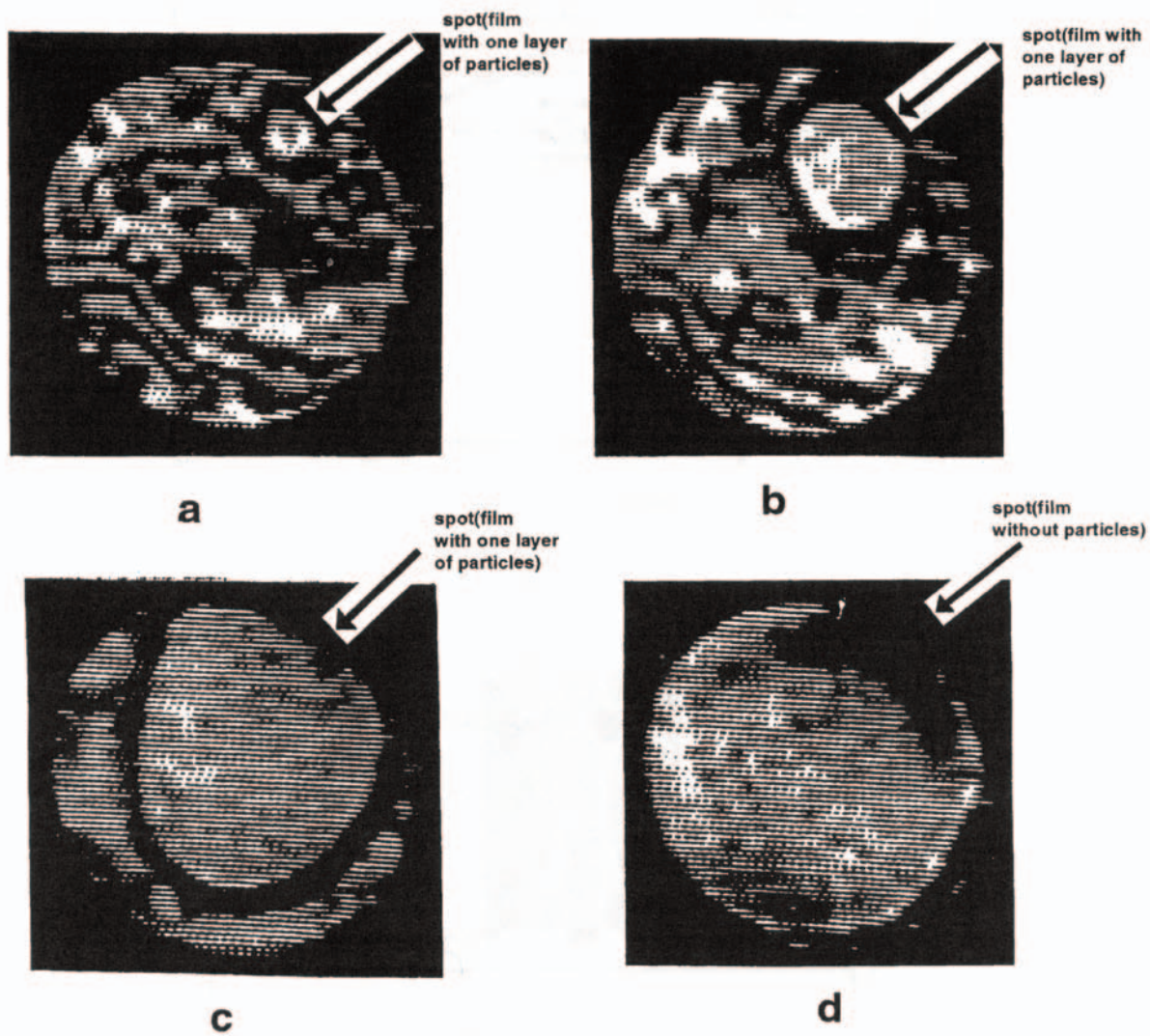
Figure 8 Sequence of photomicrographs depicting the stages of stepwise thinning of an oil emulsion film in the presence of 7 vol% asphaltene.

were D (large fat)/d (small caseinate) = 20 and the volume fraction of large particles was equal to 5 wt%. We observed that with increasing casemate concentration the structure barrier between large fat particles increased rapidly; when the caseinate concentration reached 20 vol% the structure energy barrier was larger than 3 kT. Such a high energy barrier was enough to prevent large fat-particle aggregation; therefore, the emulsion became stable. In sample 1, the caseinate submicelle concentration was estimated to be around 20 vol%. Therefore, microlayering stabilization went into effect.

We have also used the back-light scattering technique to investigate the effect of shear rate on emulsion structure. The microstructure distortions occurred at high shear rates (25).

IV. DIRECT IMAGING

This technique is particularly useful for highly concentrated emulsion systems. We have used the digitized optical imaging technique to study the microstructure of a number of
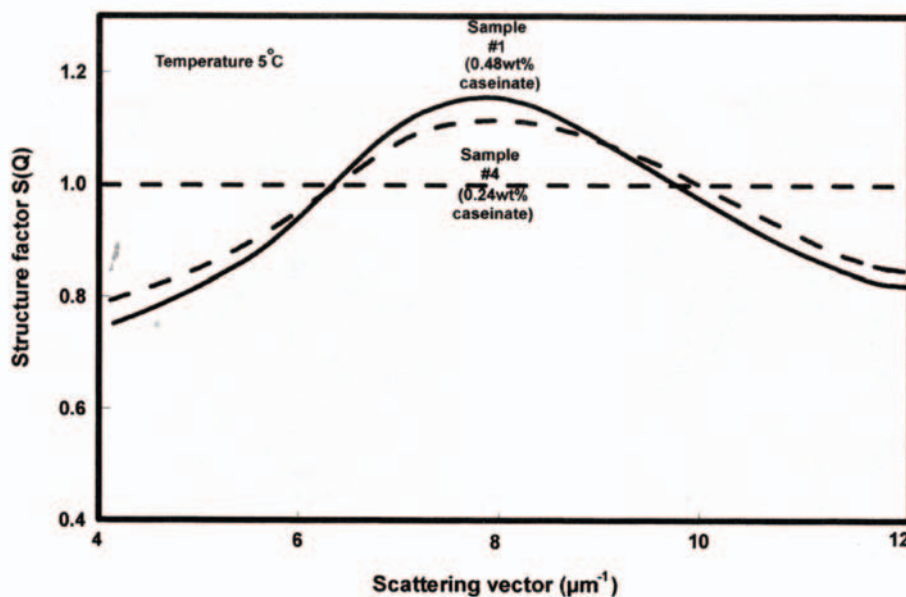
Figure 9 Effect of caseinate on fat-particle structure inside food emulsion (fat concentration: 5.14 wt%).
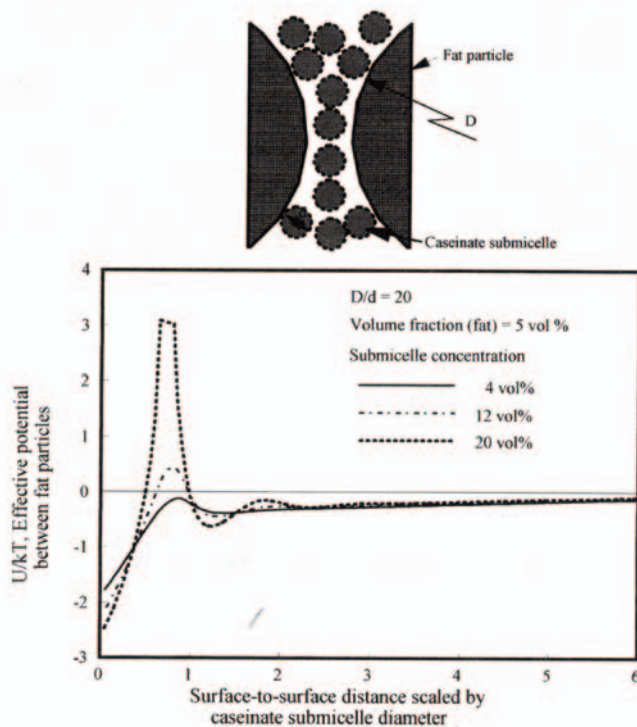

Figure 10 Stabilization mechanism of caseinate submicelle microlayering: calculated results using O-Z method (particle size ratio: 20, and fat concentration: 5 wt%).

different emulsion systems (27). In this method, an emulsion sample was taken under a microscope to record a microstructural image. This image was recorded using a video camera with imaging software (Image Pro) attached to the microscope. The microstructural image was magnified and then the analysis was done to measure the interdroplet distance. This acquired data was processed in MATLAB to calculate the radial distribution function (RDF) and structure factor. The RDF, $g(r)$, measured the probability of finding an emulsion droplet center at a distance, r, from a reference droplet. It is oscillatory in nature and tends to unity as the distance from the reference droplet tends to infinity, implying that the probability of finding a droplet at infinity is the same as that in the bulk. It typically has a maximum at a distance of one droplet diameter for a monodisperse phase system.

Figure 11 shows the $g(r)$ for two emulsion samples. The emulsion samples had the same composition, except one had sucrose ester (0.1 wt%) as the watersoluble surfactant and the other had sucrose oleate (0.1 wt%). The fat content was 40 wt%, the protein (sodium caseinate) was 4 wt%, and the water content was 56 wt%. The RDF shows that the corresponding effective pair potential of interaction between fat particles is also oscillatory. The periodicity of the curve is nearly the size of the particles. The structure factor $S(\sigma)$ for these samples is shown in Fig. 12. The first peak height of the structure factor of the sucrose oleate sample is higher, indicating that the addition of sucrose oleate facilitates the fat-particle structure formation. Thus, the fat-particle structure in the sucrose oleate sample is much

better organized than the particle structure in the sucrose ester sample. This leads to higher fat-particle flocculation in the sucrose stearate sample and the emulsion is less stable.

In summary, the nondestructive digitized imaging technique is very useful for studying structure formation in oil-water emulsion systems.

V. PIEZO IMAGING SPECTROSCOPY

This technique is based on using a piezo-transducer to monitor the process of coalescence of a drop at a liquid-liquid interface (28). A drop is formed at the tip of a capillary; the drop causes the interface to oscillate, and the oscillations of the interface are traced on a digital storage oscilloscope. The typical response of the piezo-transducer consists of an initial high-frequency (10 Hz), low-amplitude damped oscillation followed by a relatively low frequency (2 Hz), higher amplitude, highly damped oscillation (Fig. 13). The high-frequency part of the signal is attributed to film rupture while the low-frequency part is due to the formation of a jet during film drainage. Both the frequency of the signal and the damping factor are calculated from these measurements (28). This novel technique for monitoring drop/homophase coalescence in liquid-liquid dispersions having an opaque or turbid dispersion medium has been developed by us. The effects of interfacial tension, homophase viscosity, and surfactant concentration in the dispersion on the coalescence process have been studied. Several other
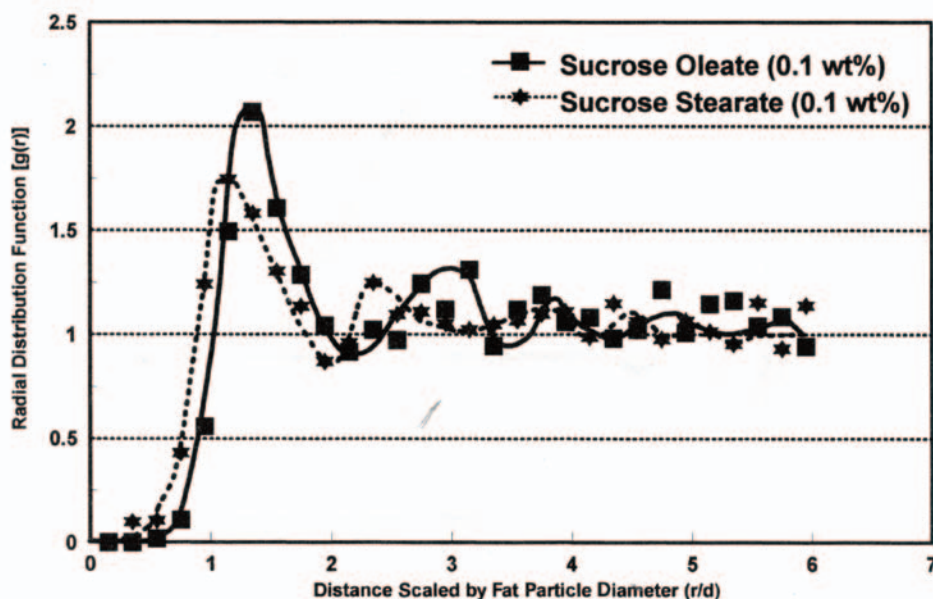

Figure 11 Effect of surfactant on radial distribution function of fat particles in oil-in-water emulsion.
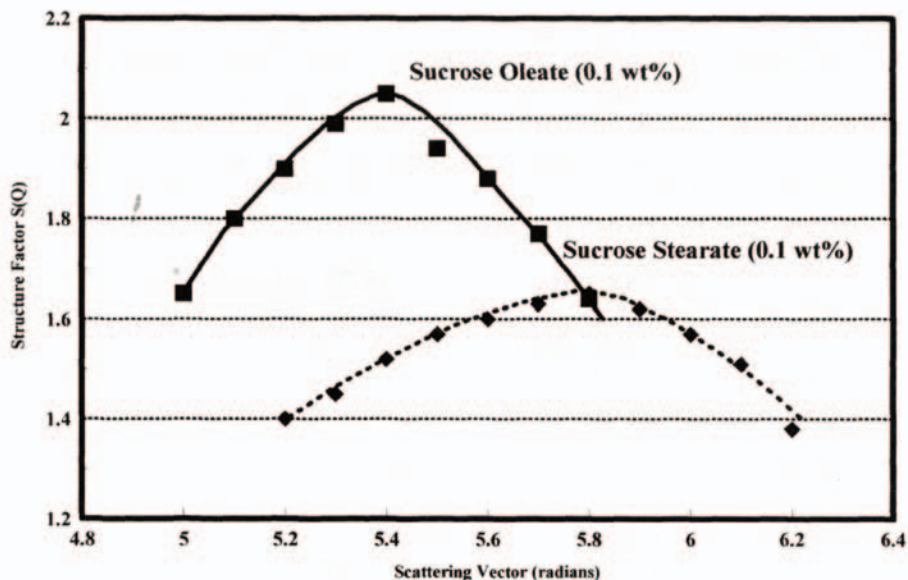
Figure 12 Effect of surfactant on structure factor of fat particles in oil-in-water emulsion.

potential applications of this technique such as measuring the rate of phase separation are also discussed by us elsewhere (28).

VI. SUMMARY

The research discussed above is based on the work performed in our laboratory in the subject area of emulsion microstructure and stability. A critical thrust of our ongoing research program has been the development of instrumental techniques for understanding the mechanism of emulsion stability in various systems including food, pharmaceutical, cosmetic, and petroleum emulsions. The development of reliable measurement techniques has been followed up by us in a series of studies, both theoretical and experimental, which were aimed at understanding the role
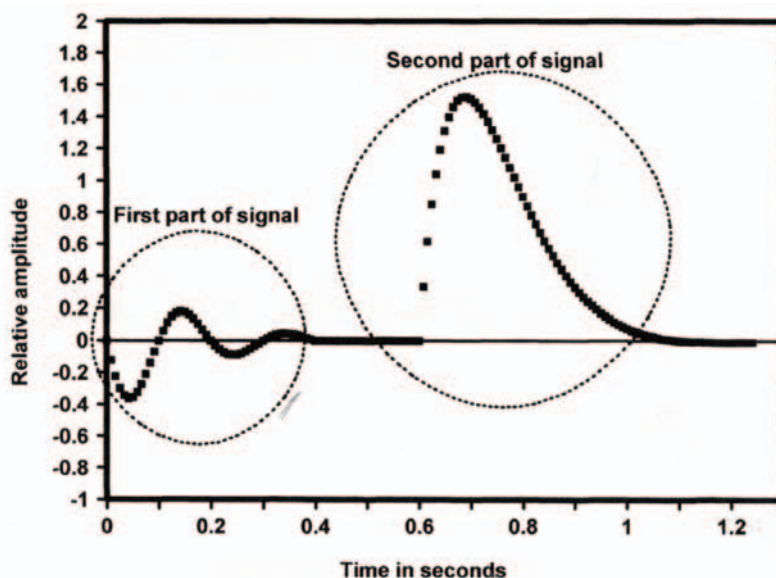

Figure 13 Typical transducer response to droplet-fat interface coalescence.

of dynamic interfacial properties in the stability of thin liquid films associated with drops and bubbles, as in emulsion and foam systems (29).

We have developed a capillary force balance to study the phenomenon of nano-sized particle/micelle structuring inside the thin liquid films, the so-called emulsion and foam films, and discovered the presence of long-range (nonDLVO) oscillatory structural forces (oscillatory disjoining pressures) induced by the confined boundaries of the film with fluid surfaces. We carried out a theoretical analysis of these forces using the statistical mechanics approach and Monte Carlo simulations. At low micelle/particle concentrations, the longrange oscillatory structural force leads to an attractive depletion effect which gives rise to phase separation in emulsions and other colloidal dispersions. However, at high micelle/particle concentrations, the oscillatory structural force induces micelle/particle structural transitions inside the film and the formation of two-dimensional crystalline layers with hexagonal interplanar ordering which offers a new mechanism for stabilizing emulsions, particle dispersions and foams. We have used both nondestructive back-light scattering and direct optical imaging techniques to characterize quantitatively these long-range structural forces in supramolecular fluids such as concentrated suspensions of nanosized particles, surfactant micellar solutions and microemulsions, and in systems of fat particles, emulsifiers, and gums (hydrocolloids). This discovery of oscillatory structural forces with a period of oscillation equal to the effective size of the micelle/particle arising from the self-organization of nano-sized particles has opened up new vistas in emulsion/dispersion science and technology. Our work on the thinning of emulsion and foam films provides a theoretical link between oscillatory disjoining pressure in thin films and oscillatory structural and depletion forces in concentrated suspensions.

ACKNOWLEDGMENTS

REFERENCES

1. D Edwards, H Brenner, DT Wasan. Interfacial Transport Processes and Rheology. Boston: Butterworth-Heinemann, 1991, pp 1—558.
2. AD Nikolov, DT Wasan. In: AT Hubbard, ed. Handbook of Surface Imaging and Visualization. Boca Raton, FL: CRC Press, 1995, pp 209—214.
3. PJ Breen, DT Wasan, YH Kim, AD Nikolov, CS Shetty. In: J. Sjöblom, ed. Emulsions and Emulsion Stability. New York: Marcel Dekker, 1996, pp 237—286.
4. DT Wasan, AD Nikolov. Emulsion Stability Mechanisms. Proceedings of the First World Congress on Emulsions, Paris, 1993, pp 93—112.
5. YH Kim, DT Wasan, PJ Breen. Colloids Surfaces 95: 235—247, 1995.
6. YH Kim, AD Nikolov, DT Wasan, H Diaz-Arauzo, CS Shetty. J Dispersion Sci Technol 17: 33—53, 1996.
7. YH Kim, K Koczo, DT Wasan. J Colloid Interface Sci 187: 29—44, 1997.
8. R Nagarajan, DT Wasan. J Colloid Interface Sci 159: 164—173, 1993.
9. JM Soos, K Koczo, E Erdos, DT Wassan. Rev Sci Instrum 65: 3555—3562, 1994.
10. R Nagarajan, K Koczo, E Erdos, DT Wasan. AIChE J 41: 915—923, 1995.
11. ED Manev, SV Sazdanova, DT Wasan. J Dispersion Sci Technol 5: 111, 1984.
12. AD Nikolov, DT Wasan. J Colloid Interface Sci 133: 1—12, 1989.
13. K Koczo, AD Nikolov, DT Wasan, RP Borwankar, A Gonsalves. J Colloid Interface Sci 178: 694—702, 1996.
14. AD Nikolov, DT Wasan. Powder Technol 88: 299—304, 1996.
15. AD Nikolov, DT Wasan. Colloids Surfaces 123/124: 375—381, 1997.
16. AD Nikolov, DT Wasan. Colloids Surfaces 128: 243—253, 1997.
17. DT Wasan. Chem Eng Ed. Spring Issue: 104, 1992.
18. DT Wasan, AD Nikolov, P Kralchevsky, IB Ivanov. Colloids Surfaces 67: 139—145, 1992.
19. AD Nikolov, PA Kralchevsky, IB Ivanov, DT Wasan. J Colloid Interface Sci 133: 13, 1989.
20. AD Nikolov, DT Wassan. Langmuir 8: 2985—2994, 1992.
21. XL Chu, AD Nikolov, DT Wasan. Langmuir 10: 4403—4408, 1994.
22. XL Chu, AD Nikolov, DT Wasan. Langmuir 12: 5004—5010, 1996.
23. XL Chu, AD Nikolov, DT Wasan. J Chem Phys 103: 6653—6661, 1995.
24. DT Wasan, AD Nikolov In: S Manne and G Warr, eds. Supramolecular Structure in Confined Geometries. ACS Symposium Series No. 736, 1999, pp 40—53.
25. W Xu, AD Nikolov, DT Wasan, A Gonsalves, R Borwankar. J Food Sci 63: 183—188, 1998.

26. W Xu, AD Nikolov, DT Wasan. J Colloid Interface Sci 191: 471—481, 1997.
27. K Kumar, AD Nikolov, DT Wasan. In: K Mittal and P Kumar, eds. Emulsions, Foams and Thin Films, New York: Marcel Dekker, 2000, pp 87—104.
28 J Chatterjee, AD Nikolov, DT Wasan. Ind Eng Chem Res 35: 2933—2938, 1996.
29. DT Wasan. In: K Mittal and P Kumar, eds. Emulsions, Foams and Thin Films, New York: Marcel Dekker, 2000, pp 1—30.